Active control of the H-mode transition on MAST

H. Meyer, Y. Andrew, P. G. Carolan, G. Cunningham, A. R. Field, A. Kirk, P. Molchanov†, V. Rozhansky†, S. Voskoboynikov† and the MAST and NBI Teams

EURATOM/UKAEA Fusion Association, Culham Science Centre, Abingdon, Oxfordshire, OX14 3DB, UK

† *St.Petersburg State Polytechnical University, Polytechnicheskaya 29, St.Petersburg, Russia*

Introduction: Future large magnetic confinement fusion devices, such as power plants, will benefit from H-mode regimes with an edge transport barrier (ETB), because of the higher energy confinement. Unfortunately, the strong gradients inside an ETB often cause instabilities, such as edge localised modes (ELM), which are not compatible with today's plasma facing components. Nevertheless, in the absence of ELMs the particle transport may be insufficient for the helium exhaust. Therefore, current research focuses on the development of small ELM regimes or active ELM control. The active control of the transition between low confinement L-mode and high confinement H-mode (with ETB) may provide an alternative approach.

Presently, for the lack of theoretical understanding, the criteria for accessing H-mode is cast into an empirical scaling law for the threshold power, $P_{\rm th}$ in MW [1]

$$P_{\rm loss} > P_{\rm th} = 0.072 \times |B|_{\rm out}^{0.7} \times \bar{n}_{20}^{0.7} \times S^{0.9} \times \left(\frac{Z_{\rm eff}}{2}\right)^{0.7} \times F(A)^{\gamma}, \qquad (1)$$

to estimate the heating requirements for future devices. Here, $P_{\rm loss}$ (MW) is the power flowing through the last closed flux surface (LCFS), $|B|_{\rm out}$ (T) the modulus of the magnetic field at the outer mid-plane (low-field-side, LFS), $\bar{n}_{20} = \bar{n}_{\rm e}/(10^{20}\ {\rm m}^{-3})$ the normalised line averaged density, S (m^2) the plasma surface area, and $F(A) = 0.1A/(1-\sqrt{2/(1+A)})$ ($\gamma = 0.5 \pm 0.5$, $A = R/a$: aspect ratio) a correction related to the trapped particle fraction. None of the parameters encompassed in this scaling law is suitable for active control.

The scaling law describes only a very limited subset of parameters affecting H-mode access. Clearly, local parameters are important for the formation of the ETB. In particular the radial electric field at the edge, E_r is important. H-mode access is very sensitive to changes in the magnetic configuration. For example, it is well established, that in single null (SN) diverted configurations the position of the X-point with respect to the ion ∇B-drift is important. With the ion ∇B-drift pointing towards the X-point $P_{\rm th}$ is reduced by up to a factor of four. More recently it has also been shown that a reduction of $P_{\rm th}$ can be achieved in double null (DN) configuration, if the two X-points are almost on the same flux surface [2, 3]. This effect is more pronounced in spherical tokamaks such as MAST and NSTX, than in conventional tokamaks such as ASDEX Upgrade [3]. The vertical position of the active X-point with respect to the divertor plate also affects $P_{\rm th}$. On JET a reduction of $P_{\rm th}$ by a factor of two has been observed during a scan of the X-point height [4]. Furthermore, plasma fuelling might provide the means of active control. For example, H-mode is facilitated by fuelling from the high-field-side (HFS) mid-plane, rather than from the LFS [5, 6]. Strong LFS fuelling can induce an H/L transition [7], as reducing the fuelling may trigger an L/H transition. H-mode can also be initiated by the density wave due to pellet injection [8]. Large pellets, however, may destroy the H-mode.

Control techniques close to DN: MAST usually operates in DN, where H-mode access is easiest. The most sensitive control is achieved by changing the radial separation of the two flux surfaces passing through each X-point at the LFS mid-plane $\delta r_{\rm sep} = r_l - r_u$. Here, $r_{l,u}$ is the radial position projected to the LFS mid-plane of the flux surface passing through lower and upper X-point respectively. The ion ∇B-drift is usually downward on MAST. In connected DN (C-DN) $P_{\rm th}$ is reduced by at least a factor of 2 compared to SN with the in ∇B-drift toward the X-point [2], if

$$|\delta r_{\rm sep}| < \frac{\rho_{\rm i}}{2} \approx \frac{\rho_{\rm i,pol}}{2} \approx \frac{\lambda_{\rm SOL}}{2} \approx 3\ {\rm mm} \qquad (2)$$

Here, $\rho_i \approx 6$ mm is the ion Larmor radius, $\rho_{i,pol} \approx 9$ mm the poloidal Larmor radius, and $\lambda_{SOL} \approx 8$ mm the scrape-off-layer (SOL) decay length. On ASDEX Upgrade P_{th} is reduced by 20% in C-DN [3].

The vertical feed back coils (P6) allow very fine control of the vertical position. The coil response time due to the time constant of the coil casing is $\tau_{P6} < 3$ ms, as can be seen from (a) in Fig. 1. The plasma is moved slightly upward and δr_{sep} (b) is changed by $\Delta\delta r_{sep} \approx 10$ mm. This induces L-mode periods of $\Delta t <$ 20 ms into, what was, an otherwise ELM free H-mode. Moving the plasma initially downward triggers an ELM. Faster downward movements are currently not possible because of the power supply protection mechanism. Smaller deviations $\delta r_{sep} < 8$ mm (Fig. 1 right) fail to introduce H-L-H phases as the shot evolves. Nevertheless, a small degradation of the density gradient (d) may still be present.

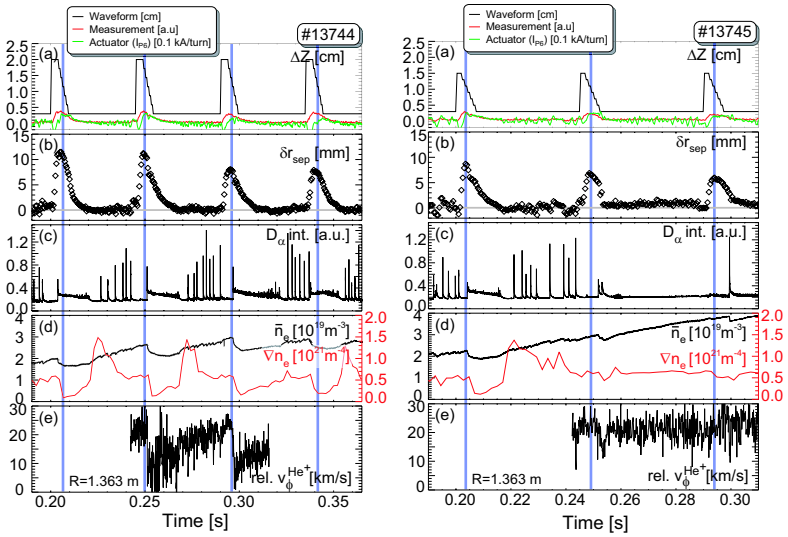

Figure 1: *H-L-H phases induced by δr_{sep} changes. (a) control waveforms and coil response, (b) δr_{sep}, (c) D_α-intensity, (d) line averaged density and density gradient, (e) toroidal velocity of HeII. In shot #13744 (left) larger deviations were programmed than in shot #13745 (right).*

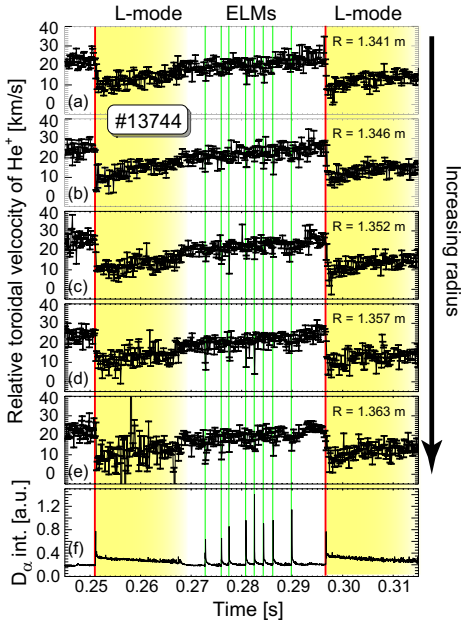

Figure 2: *Evolution of the toroidal HeII velocity during forced H-L-H phases at different radii (a-e), D_α intensity (f).*

At the H/L transition the toroidal HeII velocity decreases by $\Delta v_\phi^{HeII} \approx -20$ km/s within $\Delta t \approx (300 \pm 100)$ μs. Thereafter v_ϕ^{HeII} increases with decreasing δr_{sep}. At the L/H transition the outermost channels (Fig. 2c–e) show an abrupt increase of v_ϕ^{HeII} by about 5 km/s. This evolution is consistent with the collapse and subsequent recovery of the negative radial electric field present in H-mode. During the ELMs v_ϕ^{HeII} also decreases in the outboard channels, but this is not observed for all ELMs further inward. The time resolution of the velocity measurement is $\Delta t_m = 130$ μs, and averages typically over 2–3 ELM filaments, and generally the collapse of E_r is observed at every ELM.

The physics of the higher threshold power in SN compared to DN is probably related to the change of the SOL flow pattern. In L-mode discharges, a difference of $\Delta E_r \approx -1$ kV/m between C-DN and SN with the ion ∇B-drift towards the X-point (L-SN) has been observed on MAST and ASDEX Upgrade [3]. A larger change of E_r is observed between the two SN configurations with opposite ∇B-drift direction (L-SN and U-SN). These variations of E_r agree well with B2SOLPS5.0 simulations [9]. Other profiles, such as electron and ion temperature, or density, at the edge stay the same. The change of the SOL flow pattern is evident from the reversal of the parallel HeII flow in the HFS SOL in L-mode recently measured on MAST using localised Doppler spectroscopy (Fig. 3).

Control techniques for SN: The above technique is most feasible for spherical tokamaks, where this effect is strong, and which operate usually in DN because of the better power handling. Conventional tokamaks operate mostly in SN, although at higher triangularity δr_{sep} is decreased, and small (type-II) ELM regimes are observed close to DN.

In SN the length of the outer divertor leg can be used to control the ETB. As can be seen from Fig. 4 consecutive H-L-H phases were induced in an H-mode in SN configuration by changing the connection length of the outer divertor leg by $\Delta L_c = 2 \cdots 4$ m. The different phases are clearly visible in the D_α light (a). With the shorter connection length (divertor config. 1, top left; dark shaded phase) the plasma is in H-mode, and with the longer leg (divertor config. 2; top right) the plasma is in L-mode. Trace (b) shows the ion saturation current, j_{sat}, measured at $R = 1.015$ m, just outside shadow of the P2 plate.

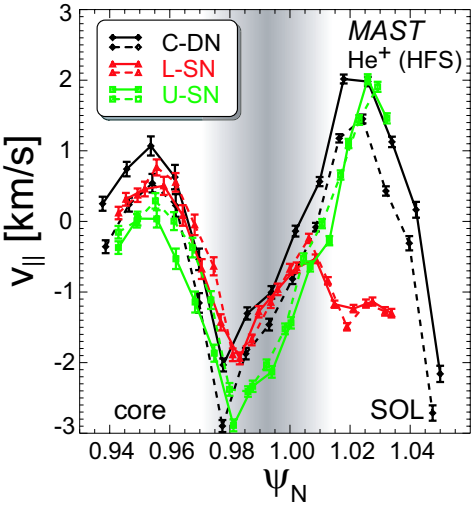

Figure 3: *Parallel flow of HeII ions at the HFS plasma edge for C-DN (black), L-SN (red) and U-SN (green) in L-mode.*

In config. 1 the strike point sits on the P2 coil protection plate, and consequently the first probe outside the shadow of the P2 plate only shows current in divertor config. 2. Once H-mode is lost, and the bootstrap current due to the steep edge gradients has vanished, the divertor leg moves inward and back onto the P2 plate, as can be seen from the reduction in j_{sat}. With the leg on the P2 plate H-mode is recovered.

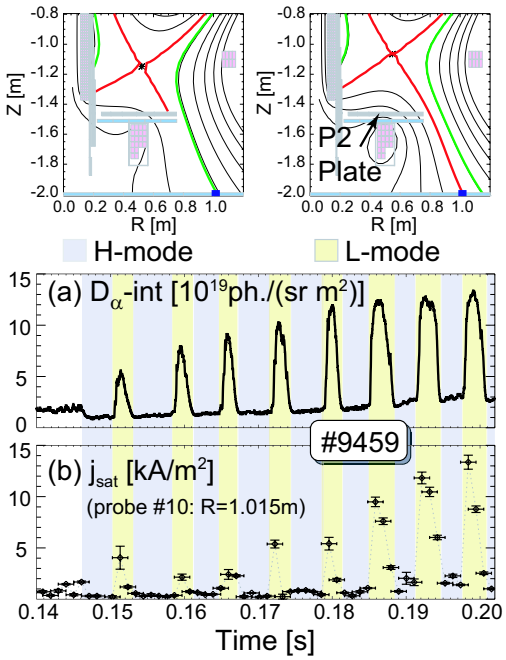

Figure 4: *Repetitive H-L-H phases induced by a change of the outer divertor leg length. The darker shaded H-mode phases correspond to the divertor configuration with the short leg (top left), the L-mode phases correspond to the long leg (top right).*

The benefit of a short outer divertor leg or a recycling closer to the X-point for H-mode access supports the JET results on divertor geometry [4]. In the X-point height scan on JET a reduction of P_{th} with X-point height was observed only when the legs were on the horizontal targets. In a similar experiment recently on MAST sustained H-mode was only obtained at similar auxiliary power in the configuration with the lowest X-point to target plate distance.

The effect of the outer divertor leg length on E_r has been modelled with B2SOLPS5.0 for an example case on MAST (#7666, Ohmic, C-DN). Some of the results of these simulations are shown in Fig. 5. The connection length from the X-point to the strike point is for the configuration with long divertor legs $L_c^{long} = 6.56$ m. For the configuration with short divertor legs it is $L_c^{short} = 5.77$ m. Hence the difference $\Delta L_c = 0.79$ m is less than $1/2$ of the one in the experimental SN case shown in Fig. 4.

Nevertheless, the modelling shows a strong reduction of the parallel velocity, $v_{||}$ at the LFS mid-plane (Fig. 5a) with shorter outer divertor legs. This is due to the reduced edge temperature in this configuration. On the one hand, the reduction in $v_{||}$ leads to a more negative E_r inside the LCFS, due to viscous coupling. The reduced temperature gradient, on the other hand, makes E_r more positive. The net effect is a slightly more negative E_r with the shorter divertor leg (Fig. 5b). In essence, the divertor configuration with the shorter divertor leg has a higher $E \times B$ shear as can be seen from Fig. 5c.

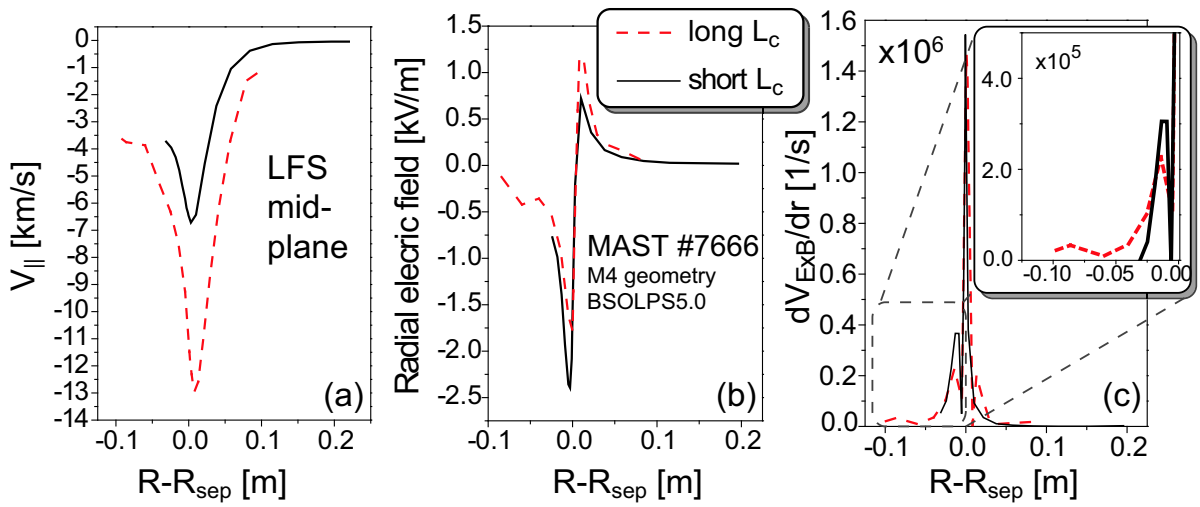

Figure 5: *B2SOLPS5.0 modelling of (a) $v_{||}$, (b) E_r, and (c) $\partial V_{E\times B}/\partial r$ at the LFS mid-plane for two different divertor leg length (long: $L_c^{\mathrm{l}} = 6.56$ m [solid], short: $L_c^{\mathrm{s}} = 5.77$ m [dashed])*

This may be the reason for the lower P_{th} in this configuration.

It is very hard to quantify the effect of the $E \times B$ shearing rate on the H-mode power threshold. The change in E_r seen in this simulation is similar to the changes observed experimentally between C-DN and L-SN discharges on MAST and ASDEX Upgrade [2, 3]. In these experiments P_{th} changed from $P_{\mathrm{th}}^{\mathrm{DN}} = 0.5$ MW in C-DN to $P_{\mathrm{th}}^{\mathrm{SN}} = 1.2$ MW in L-SN on MAST, and from $P_{\mathrm{th}}^{\mathrm{DN}} = 1.0$ MW to $P_{\mathrm{th}}^{\mathrm{SN}} = 1.2$ MW on ASDEX Upgrade.

Summary: In H-mode short, temporary back transitions to L-mode can be triggered in double null and single null by changing the magnetic configuration on MAST. In double null small upward movements of $\Delta Z_{\mathrm{mag}} \approx 1 \cdots 2$ cm ($\delta r_{\mathrm{sep}} \gtrsim 8$ mm) triggered L-mode phases of $\Delta t <$ 20 ms length. The toroidal He^+ velocity indicates a collapse of the radial electric field at the edge within 300 μs at the transition. The change of the outer divertor leg length led to L-mode phases of $\Delta t < 5$ ms in SN. In both cases modelling with B2S0LPS5.0 showed that changes of the parallel flow and temperature in the scrape-off-layer lead to a more negative electric field in the favourable configuration for H-mode. This leads to a higher $E \times B$ shear just inside the last closed flux surface, which may be the reason for the improved H-mode access. Controlling the SOL flow and perhaps details of the divertor structure could be a key for controlling the edge transport barrier in divertor tokamaks.

Acknowledgements: This work was funded jointly by the United Kingdom Engineering and Physical Sciences Research Council and by the European Communities under the contract of Association between EURATOM and UKAEA. The views and opinions expressed herein do not necessarily reflect those of the European Commission.

References:

[1] T. Takizuka *et al.*, Plasma Phys. Control. Fusion **46**(5A), A227 (2004).
[2] H. Meyer, P. G. Carolan, *et al.*, Plasma Phys. Control. Fusion **47**(6), 843 (2005).
[3] H. Meyer, P. G. Carolan, *et al.*, Nucl. Fusion **46**(1), 64 (2006).
[4] Y. Andrew, I. Coffey, *et al.*, Plasma Phys. Control. Fusion **46**(5A), A87 (2004).
[5] A. R. Field, P. G. Carolan, *et al.*, Plasma Phys. Control. Fusion **46**, 981 (2004).
[6] R. Maingi, C. S. Chang, *et al.*, Plasma Phys. Control. Fusion **46**(5A), A305 (2004).
[7] H. Meyer, P. G. Carolan, *et al.*, Czechoslovak Journal of Physics **50**(12), 1451 (2000).
[8] P. Gohil, L. R. Baylor, *et al.*, Phys. Rev. Lett. **86**, 644 (2001).
[9] V. Rozhansky, E. Kaveeva, *et al.*, in *EPS europhysics conference abstracts of the 32nd EPS Conference on Plasma Phys. and Control. Fusion* (2005), vol. 29C.